Anal Bioanal Chem (2014) 406:3985–3994
DOI 10.1007/s00216-013-7547-0

RESEARCH PAPER

# A miniature electronic nose system based on an MWNT–polymer microsensor array and a low-power signal-processing chip

**Shih-Wen Chiu · Hsiang-Chiu Wu · Ting-I Chou · Hsin Chen · Kea-Tiong Tang**

Received: 29 August 2013 / Revised: 8 November 2013 / Accepted: 2 December 2013 / Published online: 3 January 2014


**Abstract** This article introduces a power-efficient, miniature electronic nose (e-nose) system. The e-nose system primarily comprises two self-developed chips, a multiple-walled carbon nanotube (MWNT)–polymer based microsensor array, and a low-power signal-processing chip. The microsensor array was fabricated on a silicon wafer by using standard photolithography technology. The microsensor array comprised eight interdigitated electrodes surrounded by SU-8 "walls," which restrained the material–solvent liquid in a defined area of 650 × 760 μm$^2$. To achieve a reliable sensor-manufacturing process, we used a two-layer deposition method, coating the MWNTs and polymer film as the first and second layers, respectively. The low-power signal-processing chip included array data acquisition circuits and a signal-processing core. The MWNT–polymer microsensor array can directly connect with array data acquisition circuits, which comprise sensor interface circuitry and an analog-to-digital converter; the signal-processing core consists of memory and a microprocessor. The core executes the program, classifying the odor data received from the array data acquisition circuits. The low-power signal-processing chip was designed and fabricated using the Taiwan Semiconductor Manufacturing Company 0.18-μm 1P6M standard complementary metal oxide semiconductor process. The chip consumes only 1.05 mW of power at supply voltages of 1 and 1.8 V for the array data acquisition circuits and the signal-processing core, respectively. The miniature e-nose system, which used a microsensor array, a low-power signal-processing chip, and an embedded *k*-nearest-neighbor-based pattern recognition algorithm, was developed as a prototype that successfully recognized the complex odors of tincture, sorghum wine, sake, whisky, and vodka.

**Keywords** Electronic nose · Conductive microsensor array · Multiple-walled carbon nanotube · Signal-processing chip

Published in the topical collection *Chemosensors and Chemoreception* with guest editors Jong-Heun Lee and Hyung-Gi Byun.

S.-W. Chiu · T.-I. Chou · K.-T. Tang (✉)
Department of Electrical Engineering, National Tsing Hua University, Hsinchu, Taiwan
e-mail: kttang@ee.nthu.edu.tw

H.-C. Wu · H. Chen
Institute of Electronics Engineering, National Tsing Hua University, Hsinchu, Taiwan

## Introduction

Electronic nose (e-nose) systems are bio-inspired systems that imitate mammal olfaction, and have been widely used to detect gases and have been widely applied in the food industry [1], environmental monitoring [2], health care [3], and disease diagnosis [4]. In contrast to traditional gas analysis methods such as gas chromatography–mass spectrometry and Fourier transform infrared spectroscopy, e-nose systems can be of low cost, handheld, and used by nonprofessionals to identify odors [5, 6]. Although several e-nose instruments are commercially available, they are restricted by their bulky size and high price; such systems always require a laptop or desktop and are priced from US$20,000 to US$100,000. As the smart consumer electronics market has grown rapidly, the need to fabricate an ultra-low-cost, lightweight e-nose has rapidly increased, and the price of such devices is predicted to drop below US$1 by 2020 [7]. Integrated technology has advanced, allowing multiple functional components to be merged into a single chip and generate microsystems that are relevant to the gas-sensing field [8]. Microsystems demonstrate several advantages for achieving ultra-low-cost, lightweight e-nose applications, such as small sizes, light weight, efficient power use levels, low cost during mass production, and compatibility with other electronic devices such as cell phones. Similarly, e-nose systems that comprise a sensor array, interface electronics, and a processing core for pattern recognition [9] can be integrated as microsystems. In

1994, application-specific integrated circuit technology was proposed for use in sensor array interface chips to yield low-cost artificial olfaction systems [10].

The sensor array is critical to e-nose systems, and several gas sensor types have been used therein [11], such as conductivity, piezoelectric, metal oxide (MOX) semiconductor field-effect transistor, and optical sensors. The conductive sensor array is the most suitable for application in power-efficient, low-cost, miniature e-nose systems, because of its simple electrical properties and ease of operation with back-end circuits. Two conductivity sensors have been proposed, namely, conducting polymer (CP) [12] and MOX sensors [13]. In contrast to MOX sensors, CP sensors can operate at ambient temperatures, requiring no heater. Heaters consume extremely high amounts of power, reducing the battery life of battery-based e-nose devices. In addition to the power consideration, it is difficult to fabricate MOX sensors that connect with back-end complementary MOX semiconductor (CMOS) circuitry and front-end microelectromechanical systems (MEMS) [14]. By contrast, CP sensors can be simply implemented by depositing the sensing materials between two electrodes; thus, CP gas sensors are a superior choice for designing low-cost miniature e-nose systems. A CP gas sensor array was previously developed for use in handheld e-nose devices [15], comprising specific pattern-recognition hardware, such as an artificial neural network [16], and the sensor signal acquisition and processing chips required for portable artificial olfaction systems [17]. Although numerous studies have focused on miniature e-nose systems, designing and manufacturing low-cost, power-efficient systems poses a serious challenge because of the limitations of long-term data storage and poor sensor reproducibility [18]. However, the continued demand for small, cheap e-nose devices generates a need to overcome such obstacles.

This study presents a power-efficient miniature e-nose system that uses a simply structured conductive microsensor array and a signal-processing chip. The sensing film was fabricated using a controlled two-layer coating method that ensured manufacturing reliability. The sensor array can be directly connected to a signal-processing chip, which comprises two major parts (the array data acquisition circuits and the signal-processing core); the chip was fabricated using the 0.18-μm 1P6M standard CMOS process of the Taiwan Semiconductor Manufacturing Company (TSMC). Finally, a miniature e-nose prototype was designed to achieve a light, power-efficient, and wearable e-nose device. The function of the prototype was verified by testing its ability to identify complex odors, namely, those of tincture, sorghum wine, sake, whisky, and vodka.

## Experimental

The e-nose system (Fig. 1) combined two chips, a microsensor array and a low-power signal-processing chip. This two-chip

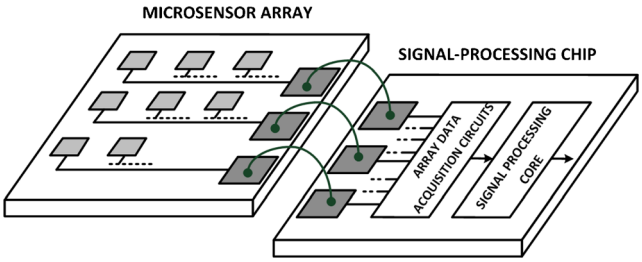


**Fig. 1** A two-chip solution for electronic nose (e-nose) systems, comprising a front-end sensor array and a back-end low-power signal-processing chip

structure facilitated the development of a miniature e-nose system. For flexibility, suitable microsensor arrays can be adopted for various applications. The novel design can incorporate most of the discrete components used in e-nose devices into the small chips, increasing the space efficiency and shrinking the size and cost of the device. The microsensor array possessed eight multiple-walled carbon nanotube (MWNT)-based sensors and was fabricated using standard photolithography technology; to reduce the complexity of the manufacturing process, no MEMS processing was used. The metal interdigitated electrodes can deposit appropriate CP-sensing materials, forming microsensors. By use of wire-bonding or packaging methods, the microsensors directly connect to the low-power signal-processing chip [17], which possesses two parts, namely, the array data acquisition circuits and the signal-processing core. The array data acquisition circuits, which connect to the microsensors, comprise eight-channel interface circuits and an analog-to-digital converter (ADC). The signal-processing core, which comprises memory and a microprocessor, receives data from the array data acquisition circuits and runs the odor classification and system operation programs.

## Conductive MWNT-based microsensor array

Although miniature MOX-based gas sensors exist, they are primarily manufactured using complex MEMS or specific processes [19]. Fortunately, CP-based gas sensors allow chemical gas sensor arrays to be fabricated using the standard photolithography process, ensuring a simple manufacturing process, small size, functionality at ambient temperatures, and low cost. Microsensors were previously implemented by depositing CP composite materials between 100-μm-wide gold leads that occupied a small area of 250×250 $\mu m^2$ on silicon [12]. The microsensor array (Fig. 2) was fabricated using standard photolithography technology. First, 10 μm of AZ9620 was spin-coated on a 700-μm-thick glass substrate, patterned using UV exposure ($\lambda$=350–450 nm), and developed using AZ400K. After development, 10 nm of chromium and 200 nm of gold were sequentially deposited using an E-gun evaporator; subsequently, a lift-off process was applied, using the solvent acetone to form the interdigitated electrode

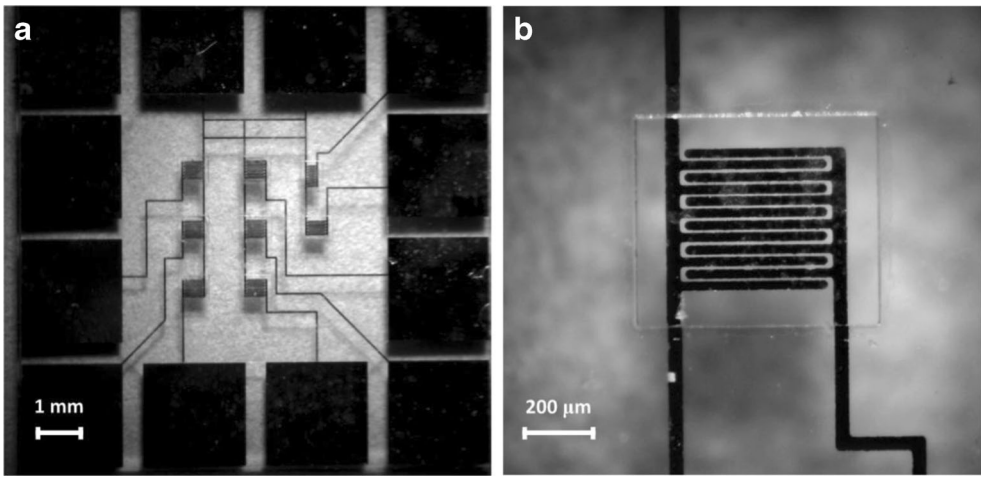


**Fig. 2** Photographs of **a** the microsensor array and **b** a single sensor element

array. After the lift-off process, 50 μm of SU-8 3050 was spun onto the interdigitated electrode array substrate, thoroughly patterning an 650×760 $\mu m^2$ rectangle. There were eight interdigitated electrodes, of which seven occupied an area of 400 × 400 $\mu m^2$ and six possessed interdigitated electrodes pairs. One of the interdigitated electrodes occupied an area of 500 × 250 $\mu m^2$ and had eight interdigitated electrode pairs. The width of the interdigitated electrode fabricated using gold was 25 μm and the spacing between the electrodes was 13 μm.

Fabricating CP microsensors generates serious challenges, including poor reproducibility and repeatability, because of the unstable coating of the composite sensing film. Furthermore, to fabricate sensor arrays, composite sensing films always comprise several distinct materials, yielding disparate effects when deposited on the same substrate type. The novel biological two-layer structure [20] was proposed, offering an efficient method for improving microsensor responses. Compared with traditional one-layer films, two-layer films yield a stabler sensing response because the polymers and conducting materials comprise distinct layers. Such processing avoids causing aggregation in the conductive material and polymer mixing solutions, particularly those required in various large sensors used in sensor arrays. Fabricating two-layer sensing film requires two steps. First, the conducting layer is coated using the conducting materials. Second, the polymer layer is coated to ensure gas selectivity. MWNTs were used in the conducting layer because of their effective performance levels regarding sensitivity, response time, reproducibility, and long-term stability in CP-based gas sensors [21]. The MWNTs were dissolved in water at concentration of 1 mg/mL (1 wt %). The solution was deposited on the interdigitated electrodes by using a nanoliter injector, and the water was driven out at 70 °C, forming the conductive film. Subsequently, polymers were selected for the second layer; the linear solvation energy relationship (LSER) theory was used [22] and the physical absorption bonding was analyzed. The LSER theory offers a basic method of selecting polymers to enhance the gas selectivity of a sensor array. LSER equations correlate the logarithm of the partition coefficient of a vapor in a polymer on the basis of the vapor solvation parameters by using a series of LSER coefficients related to the solubility properties of the polymer. A smaller solvation coefficient corresponds to a larger interaction between the gas and the polymer. For example, applying the LSER equation to estimate the solvation coefficient between ethanol gas and various polymer membranes, we can estimate the extent of adsorption as poly(methyl vinyl ether-*alt*-maleic acid)>poly(ethylene adipate)>hydroxypropyl methyl cellulose>poly(vinylbenzyl chloride). Accordingly, seven polymer composite materials were selected for deposition in the second layer for eight distinct sensors. Table 1 shows the polymers and the corresponding solvents.

## Power-efficient signal-processing chip

The microsensor array connects to the interface circuitry and the front end of the signal-processing circuit. An eight-channel adaptive interface circuitry connects to various sensors, an ADC, the memory unit, and an 8051 microprocessor. The adaptive interface circuit [23] converts the sensor signal to a voltage. Additionally, the interface circuit can adapt to the sensor to eliminate initial baseline resistance variations that

**Table 1** The polymers used in the microsensor array

| Polymer | Solvent |
|---|---|
| Poly(4-vinylphenol-*co*-methyl methacrylate) | MEK |
| Poly(vinylbenzyl chloride) | MEK |
| Poly(ethylene adipate) | MEK |
| Poly(methyl vinyl ether-*alt*-maleic acid) | $H_2O$ |
| Polyvinylpyrrolidone | $H_2O$ |
| Poly(vinylidene chloride-*co*-acrylonitrile) | MEK |
| Styrene/allyl alcohol copolymer | MEK |

*MEK* methyl ethyl ketone

result from environmental factors, such as sensitivity of the polymer to temperature and humidity, and manufacturing factors such as dispersion of the MWNTs. Before gases are sensed, the circuit adapts the sensor voltage at a preset value to ensure there is a stable baseline. After adaptation, the circuit can begin reading the sensor response signal, and the resistive changed ratio can be obtained. Then, the eight-to-one multiplexer selects one of the output signals from the eight-channel adaptive interface, and subsequently sends the signal to the ADC. The low-power 8-bit successive approximation ADC receives the analog signal and converts it into a digital signal [24]. The ADC consists of a sample-and-hold circuit with a bootstrap technique, a digital-to-analog converter, a successive approximation register (SAR), and a rail-to-rail comparator with an adaptive power control.

An 8051 microprocessor runs the program used for the system operation and gas identification algorithm. The 8051 microprocessor can be used as an embedded microcontroller to easily implement a small, low-power, inexpensive, portable e-nose [25]. The microprocessor controls the hardware, acquiring raw sensor data from the eight-channel adaptive interface circuitry and the ADC. When gas is detected, the microprocessor performs the vital preprocessing tasks, and changes the system status from "standby mode" to "data collection mode" when the sum of the resistive change of each sensor is greater than 10 %. When the sensor reaches the steady state, the system status changes from "data collection mode" to "gas identification mode." Finally, the result is exported. Simple algorithms such as nearest neighbor, $k$ nearest neighbors (KNN), linear classifiers, and quadratic classifiers, can be applied in gas identification. Static random access memory (SRAM) is used as the data memory and program memory, which store the odor database and system operation procedure. The SRAM occupies most of the chip area and consumes most of the power in the embedded system. In this SRAM, a row–column clustered sleep-transistor placement (RCCSTP) scheme [26] is used to suppress power consumption and leaking current, and to reduce the area overhead caused by sleep transistors.

## Miniature e-nose system prototype

A miniature e-nose system was developed, using the microsensor array and the low-power signal-processing chip. The off-chip components comprised only a liquid crystal display (LCD), level shifters, flash memory, power and bias modules, and an oscillator. The microsensor array can be adjusted for various applications. Because of the limitations of available CMOS technologies, the system required flash memory, which facilitated transferring the program to the on-chip memory after booting up the e-nose chip. The program comprised the system operating procedures, gas pattern classification algorithm, and odor database. The 8051 microprocessor that runs the program operation is the central unit of the system, controlling the low-power signal-processing chip, judging the sensor data, and determining the two different states: 6. standby mode and (2) gas identification mode. When an odor flows in, the system switches from standby mode to gas identification mode. When the system obtains the steady-state sensor signature, it sends signals to the gas pattern classification algorithm to facilitate odor classification. In addition, this procedure controls the LCD, displaying a real-time "fingerprint" of the operation, and subsequently, the odor classification results. Because of the distinct operational voltages of the low-power signal-processing chip and LCD, level shifters were inserted to boost the lower output voltage level from the signal-processing chip to the LCD. The power and bias modules provide the component operation bias and supply voltages. The oscillator generates a 10-MHz main reference operation frequency, which transfers to the low-power signal-processing chip, and serves as the operating frequency of the 8051 microprocessor.

The experimental setup used in [20] was applied to assess the sample-sensing properties of the proposed sensor device. To perform the experiments, the device was placed in a Teflon testing chamber. The vapor flow rate was maintained at 200 mL/min, and a KIN-TEK 670C standard gas generator was used as a vapor-generating system. The vapor flow was produced by the evaporation of a volatile solvent and the gas generator adjusted the temperature controls to manipulate the vapor concentration. The temperature was controlled between 30 and 100 °C to generate low to high vapor concentrations. During each test, the target gas was infused into the chamber for adsorption and dry air was subsequently infused for desorption at 200 mL/min. We placed the test solvent in a KIN-TEK 670C standard gas generator for 5 h and measured the weight loss of the solvent. Finally, we calculated the gas concentration by using the following equation:

$$\text{Concentration(ppm)} = \frac{MW}{22.4 \times 0.2L \times T}, \tag{1}$$

where $M$ is the molecular mass, $W$ is the weight loss of the solvent, and $T$ is the measurement time. The adsorption and desorption periods could be set using a timer to automatically switch the phase. For portable, lightweight e-nose devices, a small vacuum pump connected to a sampling bottle can replace the standard gas generator, providing a stable source of test gas.

## Results and discussion

The power-efficient miniature e-nose system consisted of the microsensor array and the signal-processing chip, integrated on a printed circuit board (PCB). The MWNT-based microsensor array was implemented after using the two-layer sensing material deposition process on the eight interdigitated electrodes

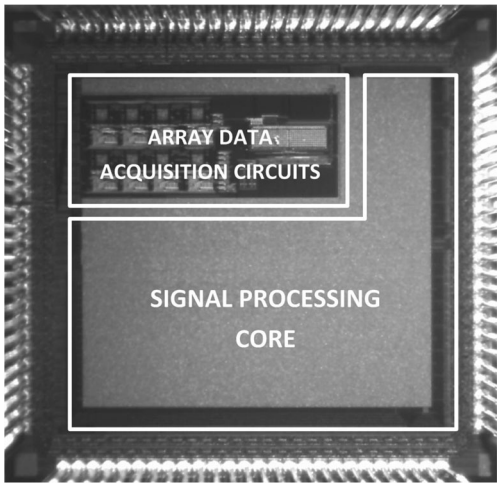


**Fig. 3** The die micrograph of the low-power signal-processing chip

(Table 1), and the low-power signal-processing chip (Fig. 3) was fabricated using the TSMC 0.18-μm 1P6M standard CMOS process. The low-power signal-processing chip occupied an area of 2,058×1,952 $\mu m^2$. Figure 3 shows a die photograph including the array data acquisition circuits and the signal-processing core. Because the signal-processing core was primarily synthesized from the standard cell, the circuits were covered by a metal compensating layer. The gas response would show the performance of the microsensor array on the basis of its ability to sense complex odors containing similar ingredients, namely, those of tincture (brewed using several Chinese herbal medicines; 27 % alcohol), sorghum wine (brewed using sorghum and wheat; 53 % alcohol), sake (brewed using rice; 13 % alcohol), whisky (brewed using corn, wheat, and barley; 40 % alcohol), and vodka (brewed using wheat; 40 % alcohol).

## Conductive MWNT-based microsensor array

For the resistive sensor, the sensor resistance determined the flicker noise behavior and the power consumption. Large resistances increased the flicker noise, whereas small resistances increased the DC power consumption [27]. After 10 min of homogeneous sonication, 10 nL of the MWNT solution was deposited as the first layer of the microsensor array. In this stage, the original resistance magnitudes of the sensor array were controlled between 1.0 and 3.0 kΩ. After the second layer of variable polymers had been deposited, the resistance magnitudes of the sensor array ranged from 3.0 to 10.0 kΩ. The performance levels were tested, using various amounts of polymer as the second layer; the testing indicated the optimal ratio of MWNTs to polymer was 1:1. Coating too much polymer would reduce the gas sensitivity, caused by the thick polymer layer. Coating too little polymer would result in a nonuniform polymer layer. The basic detection responses of the sensors were measured for the simple volatile organic compound methanol. Figure 4 shows the detection magnitude of $\Delta R/R_0$ of the MWNT–polymer sensors

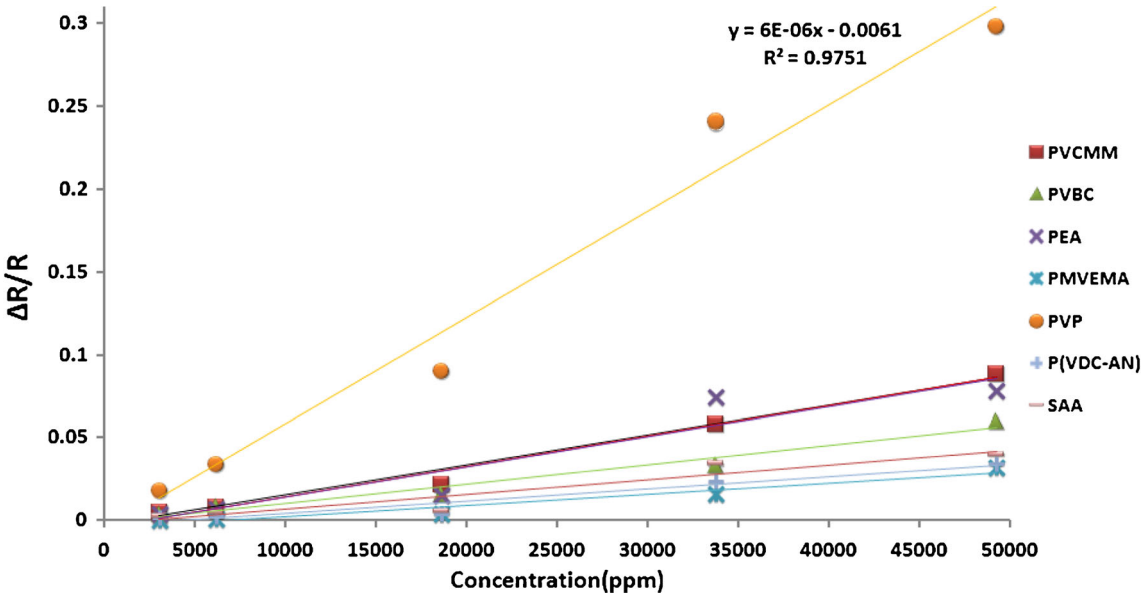


**Fig. 4** Resistance change ratio versus methanol concentration for the polymer-coated microsensors. *PEA* poly(ethylene adipate), *PMVEMA* poly(methyl vinyl ether-*alt*-maleic acid), *PVBC* poly(vinylbenzyl chloride), *PVCMM* poly(4-vinylphenol-*co*-methyl methacrylate), *P(VDC-AN)* poly(vinylidene chloride-*co*-acrylonitrile), *PVP* polyvinylpyrrolidone, *SAA* styrene/allyl alcohol copolymer

corresponding to the methanol concentration in an air-conditioned environment at 30 °C. The concentration of methanol was modulated between 1,000 and 100,000 ppm in dry air, and the relation curve shows the linearity between the concentration of methanol and the detection magnitude of the resistor. The integrated sensor exhibited a regression coefficient ($R^2$) of 0.9794 and a detection sensitivity of approximately 1,000 ppm, yielding $\Delta R/R_0$ of 0.69 %. Figure 5 shows the timing response of the sensor array with a methanol vapor concentration of 4.9 %. In the experimental setup, the odor absorption and desorption periods were regulated to 5 and 15 min, respectively. We observed that the reaction time and the recovery time were consistent. For all sensors, the reaction time to 90 % of the peak maximum was 2 min during the absorption phase, and the recovery time was 10 min to 10 % of the peak during the desorption phase. Although the variations of the reaction time and recovery time could be caused by different forces involved in binding to the test gas, the microsensor array was suitable in our system for detecting odors.

The sensor array affects the success rate of odor classification. In this case, we applied five alcohol odors (those of tincture, sorghum wine, sake, whisky, and vodka) to test the sensors. After acquiring the raw signal, we processed the data in the e-nose chip. The detection response of the percentage change in resistance was calculated according to $R_{\mathrm{det}}=\Delta R/R_0$ for each channel, and then the results were normalized to eliminate the effect of gas concentration and to obtain the odor fingerprint by using the following equation:

$$\left(R_{1,\mathrm{nor}}, R_{2,\mathrm{nor}}, \ldots, R_{n,\mathrm{nor}}\right) = \left(\frac{R_1}{R_1+R_2+\cdots+R_n}, \frac{R_2}{R_1+R_2+\cdots+R_n}, \ldots, \frac{R_n}{R_1+R_2+\cdots+R_n}\right). \quad (2)$$

The bar chart in Fig. 6 shows the odor fingerprints of tincture, sorghum wine, sake, whisky, and vodka. We obtained 25 sampling points for each type of beverage. Although the fingerprints were similar because the ingredients were similar, we distinguished the slight differences between odors by maintaining small variations in the data. The highest standard deviation was approximately 0.018 in this data set. Furthermore, Fig. 7 shows the principal component analysis (PCA) results in two dimensions, PCA1 (64.45 %) and PCA2 (30.31 %). The clustering demonstrated the well-defined boundaries between these five odors groups, which could be identified using a simple classifier, such as KNN, in the low-power signal processing chip.

## Power-efficient signal-processing chip

Table 2 summarizes the specifications and performance of the low-power signal-processing chip, which was measured at 1.0 V and 1.8 V for the array data acquisition circuits and the signal processing core, respectively. Compared

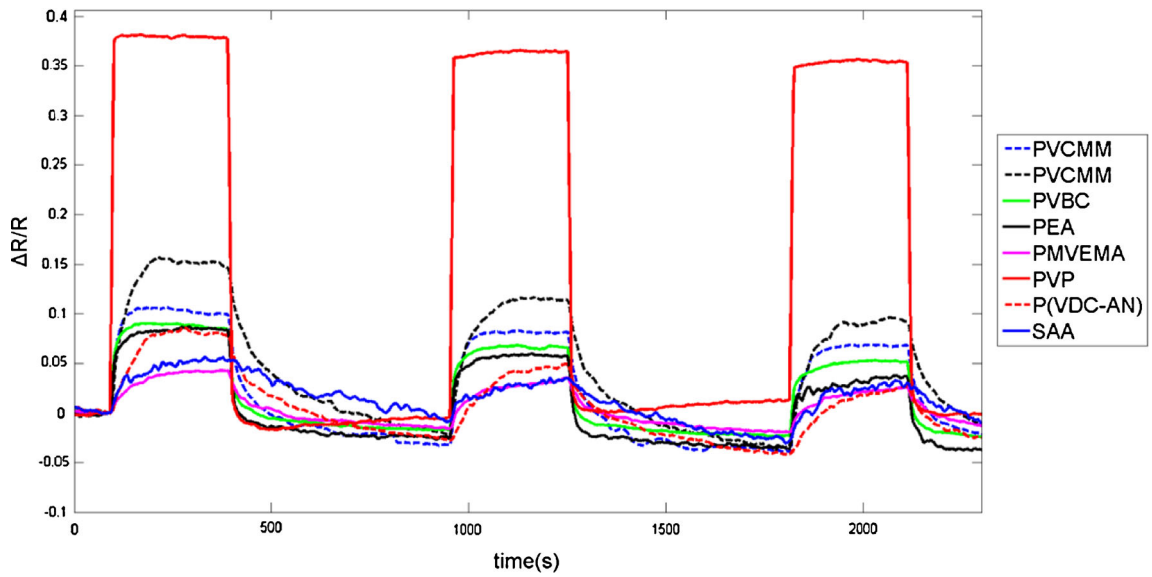


**Fig. 5** Three consecutive gas sensing responses of the microsensor array to methanol gas

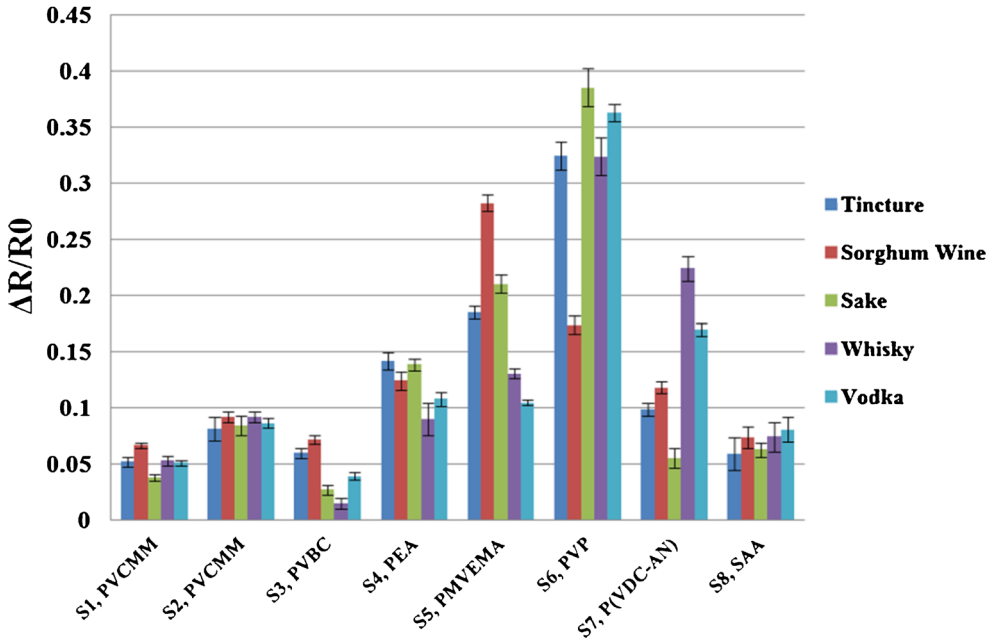


**Fig. 6** The collective response of the sensor array for five alcohol odors: those of tincture, sorghum wine, sake, whisky, and vodka

with the traditional 1.8-V supply voltage for array data acquisition circuits, the lower supply voltage design reduced the power consumption by approximately 66 % by reducing the DC power required to operate the conductive sensors. Because the CP-type gas sensor exhibits severe initial resistance drift owing to temperature, humidity, and process variation, the adaptive interface circuit is required to read out a wide range of resistance values for other conductive sensor arrays. The proposed adaptive interface automatically adjusts the sensor supply current to obtain resistance ranges from 1 kΩ to 1.5 MΩ. At a 1-V supply voltage, the interface consumes only 53.4 μW and 96.6 μW when encountering the 10-kΩ and 1.5-MΩ resistances, respectively. Converting the analog sensor signal to a digital signal, a low-power SAR ADC measured a 0.7/-0.8 least significant bit of differential nonlinearity and a 1.9/-1.2 least significant bit of integral nonlinearity at a 100-kHz input signal and a sampling rate of 250 kS/s. The resulting effective number of bits (ENOB) was 7.06, and the power consumption of the SAR ADC was 2.86 μW at a 1-V system supply voltage. The figure of merit ($P/f_s 2^{ENOB}$) of the low-power SAR ADC is 85.7 f. per conversion step. Regarding the

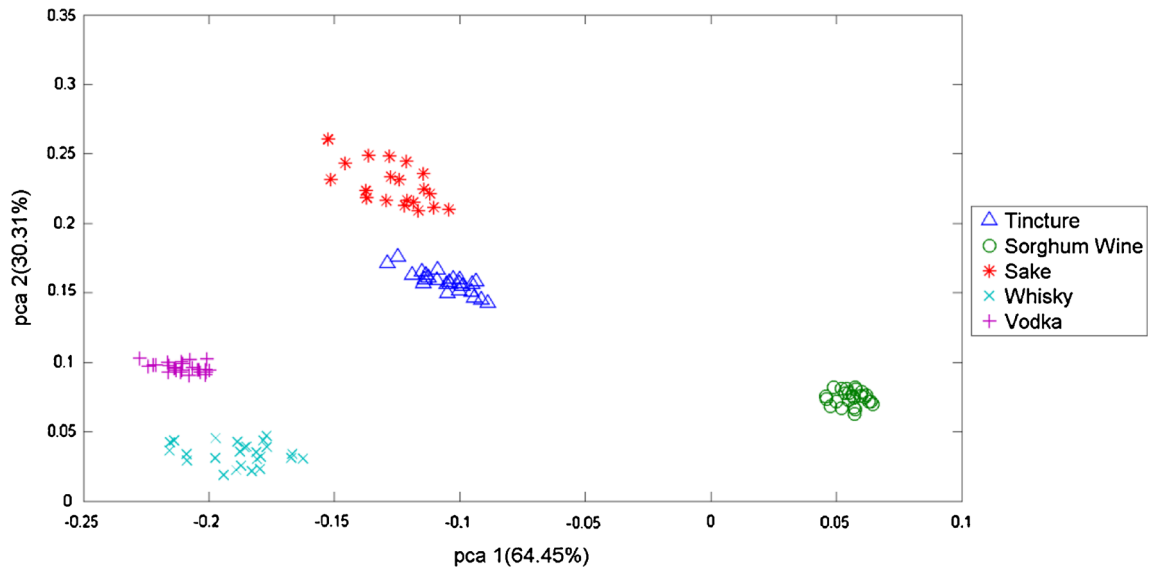


**Fig. 7** A 3D projection of the principal component analysis (*pca*) results for five alcohol odors; a clear boundary is evident between each group

**Table 2** Summary of the electronic nose chip specifications and performance

| | |
|---|---|
| Microsensor array | |
| Sensor type | MWNT–polymer |
| Disposition technology | 2-layer coating method |
| Material of conducting layer | MWNT |
| Sensor size (quantity) | 400 × 400 $\mu m^2$ (7), 500 × 250 $\mu m^2$ (1) |
| Sensing concentration | >1,000 ppm |
| Relative resistance change | >0.5 % |
| Electronic nose chip | |
| Technology | TSMC 0.18 μm CMOS 1P6M |
| Supply voltage | 1.8 V /1 V |
| Total power consumption | 1.05 mW |
| Total area | 2,058 × 1,952 $\mu m^2$ |
| Adaptive interface circuit | |
| Minimum power consumption ($R_s$=10 kΩ) | 53.4 μW |
| Maximum power consumption ($R_s$=1.5 MΩ) | 111.4 μW |
| SAR ADC | |
| Resolution | 8 bits |
| DNL | 0.7/-0.8 LSB |
| INL | 1.9/-1.2 LSB |
| ENOB ($f_s$=250 kS/s , $f_{in}$=100 kHz) | 7.06 bits |
| Power consumption ($f_s$=250 kS/s) | 5.14 μW |
| FOM | 85.7 fJ/conversion step |
| SRAM | |
| Type | 6 T SRAM |
| Maximum operation speed | 150 MHz |
| Capacity | 16 K word, 8 bits per word (128 kilobits) |
| Dynamic power | 0.109 mW/MHz (16.47 mW at 150 MHz) |
| Standby current in normal mode (1.8 V)/sleep mode (0.6 V) | 3.62 μA/0.95 μA |

*ADC* analog-to-digital converter, *CMOS* complementary metal oxide semiconductor, *DNL* differential nonlinearity, *ENOB* effective number of bits, *FOM* figure of merit, *INL* integral nonlinearity, *LSB* least significant bit, *MCNT* multiple-walled carbon nanotube, *SAR* successive approximation register, *SRAM* static random access memory, *TSMC* Taiwan Semiconductor Manufacturing Company

power efficiency, the reduction efficiency was 68 % at a sampling rate of 250 kS/s, and could reach 80 % at a rate of 125 kS/s. The 8051 microprocessor is an 8-bit complex instruction set computing microprocessor, which is compiled using an open-source Verilog code, and operates the KNN algorithm for identifying odors and controlling system procedures. The 128-kilobit RCCSTP SRAM was used as external supplemental memory for the microprocessor. The RCCSTP SRAM macros have a zero area penalty compared with that of a compact-area regular SRAM macro, which is 12–74 % smaller than that of a commercial standard SRAM compiler. In addition, the RCCSTP SRAM macros reduce the standby current by approximately 69–78 % in compared with the normal mode for the measured samples in sleep mode.

At operational voltages of 1.0 and 1.8 V, the array data acquisition circuits and the signal-processing core occupied core chip areas of 18 % and 82 %, respectively, and their power consumption was measured to be 35 % and 65 %, respectively. When both voltages were 1.8 V, the array data acquisition circuits and signal-processing core operated at power consumption ratios of 78 % and 22 %, respectively. This was primarily because DC power was consumed through the sensors in the interface circuit. Thus, the interface circuit consumed power critical for the e-nose chip and we designed the system to operate at a low supply voltage to reduce power consumption.

## Miniature e-nose system prototype

Figure 8 shows the miniature e-nose system prototype, which was based on the self-developed MWNT–polymer microsensor array and low-power signal-processing chip; these components were assembled together with discrete components in the PCB, namely, a 16 character × two line LCD (LMC-SSC2A16-01), level shifters, a 32-megabit flash memory component (AT49SV322D), power and bias modules (L7805CV, LD1117A), and a 10-MHz crystal oscillator (MCO-1500A). A testing chamber was designed to contain the microsensor array, and the test gas was delivered into the chamber using a 0.125-in. tube. The PCB had a volume of 9.5 × 9.5 × 2.2 $cm^3$, and its weight was only 137.8 g including the

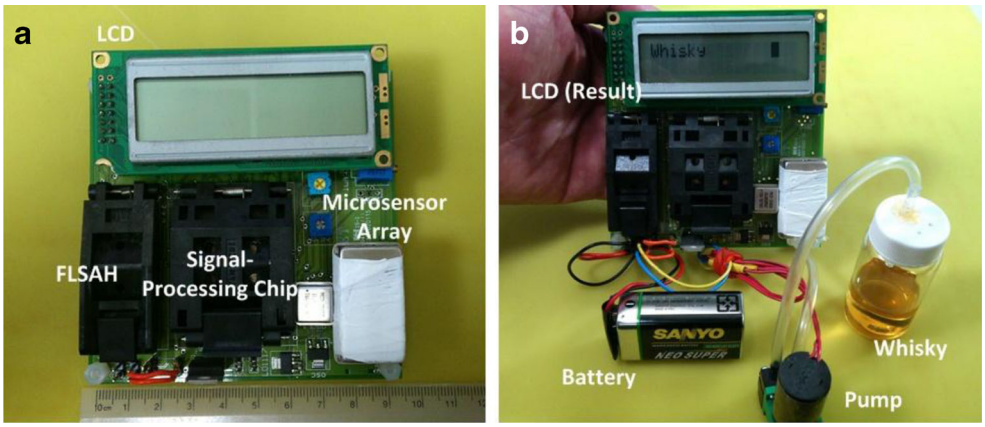


**Fig. 8** The miniature e-nose device prototype

LCD. Finally, the testing chamber was connected to a small diaphragm pump (THOMAS® 2002 model, 25 mA at 5 V), which delivered the test gas from the sampling bottle. The e-nose prototype was operated using a 9-V battery and the power modules converted the 9 V to 5 V and 1.8 V. If the supply voltage to the diaphragm pump and LCD is ignored, the proposed e-nose system can be operated at low supply voltages and consumed little power. The prototype demonstrated its odor classification functionality. After programming the KNN algorithm and embedding the odor database in the software, we conducted an odor test. The proposed system achieved 100 % accuracy, identifying tincture, sorghum wine, sake, whisky, and vodka.

## Conclusion

We designed and implemented an e-nose system that used an MWNT-based microsensor array and a low-power signal-processing chip. The two-chip structure facilitated the fabrication of the miniature system. The microsensor array integrated eight sensors by using standard photolithography technology and the sensing materials were deposited using a reliable two-layer coating method. The microsensor array is advantageously designed, detecting and identifying volatile organic compounds and odors that exhibit complex compositions. The front-end microsensor array can directly connect with the back-end low-power signal-processing chip, which comprised data acquisition circuits and a signal-processing core. The chip was fabricated using the TSMC 0.18-μm 1P6M standard CMOS process. The resulting device occupied a small area and consumed little power. By using these chips, we fabricated a miniature e-nose prototype. In the prototype, the microsensor array can be adjusted in various applications, and classification algorithms and odor databases were included in the memory unit. Table 3 shows a comparison of the portable e-nose systems. We designed a smaller e-nose system compared with other documented portable e-nose systems because integration technology was required for the sensor array and signal-processing chip. Compared with [15], we

**Table 3** Comparison of portable electronic nose systems

| | Kim et al. [15] | Tang et al. [28] | Wang et al. [20] | This work |
|---|---|---|---|---|
| System power supply | NA | 12 V | 18 V | 9 V |
| Size | Sensing module, 5×7 $cm^2$, plus laptop, PC, or PDA | Individual device, 20×12×10 $cm^3$ | Individual device, 28×18×12 $cm^3$ | Individual device, 9.5 × 9.5 × 2.2 $cm^3$ |
| Weight | NA | 1,780 g | 540 g | 137.8 g |
| Sensor technology | Carbon black–polymer composite | Commercial metal oxides | 2-layer MWNT–polymer | 2-layer MWNT–polymer |
| Channels | 13 | 8 | 8 | 8 |
| Sensor array | Single chip | Discrete sensors | Single chip | Single chip |
| Sensor interface<br>Processing unit | Discrete component<br>Laptop, PC/PDA | Discrete component<br>8051 microprocessor, learning board | Discrete component<br>8051 microprocessor, discrete component | Specific signal-processing chip, including 8051 microprocessor |
| Power consumption | Medium | High | Medium | Low |
| Portability | High | Low | Medium | High |

*NA* not available, *PC* personal computer, *PDA* personal digital assistant

implemented the system without using a personal digital assistant or personal computer to conduct signal processing. Compared with [28], we adapted a microsensor array to replace the discrete MOX sensor array, which can reduce the power consumption and device volume. Compared with [20], we implemented the system by using a single signal-processing chip to replace the discrete components. To verify the feasibility of the system, the prototype was tested and successfully classified the complex odors of tincture, sorghum wine, sake, whisky, and vodka. By using the KNN algorithm, we attained 100 % accuracy.

**Acknowledgments** The authors acknowledge the Chung-Shan Institute of Science and Technology, Taiwan, for its technology consulting support and the National Science Council of Taiwan for its financial support (NSC 102-2220-E-007-006). The authors also thank Hung-Yi Hsieh, Meng-Fan Chang, Chih-Cheng Hsieh, and Jyuo-Min Shyu from National Tsing Hua University for chip design collaboration, and Li-Chun Wang from Chung-Shan Institute of Science and Technology for sensor design consulting.

## References

1. Herrmann U, Jonischkeit T, Bargon J, Hahn U, Li Q-Y, Schalley C, Vogel E, Vögtle F (2002) Monitoring apple flavor by use of quartz microbalances. Anal Bioanal Chem 372(5–6):611–614
2. De Vito S, Massera E, Di Francia G, Ambrosino C, Di Palma P, Magliulo V (2011) Development of an e-nose solution for landfill and industrial areas emission monitoring: selection of an ad-hoc sensor array. In: Neri G, Donato N, d'Amico A, Di Natale C (eds) Sensors and microsystems. Lecture notes in electrical engineering, vol 91. Springer, Dordrecht, pp 373–377
3. Voss A, Baier V, Reisch R, Roda K, Elsner P, Ahlers H, Stein G (2005) Smelling renal dysfunction via electronic nose. Ann Biomed Eng 33(5):656–660
4. Dutta R, Hines E, Gardner J, Boilot P (2002) Bacteria classification using Cyranose 320 electronic nose. Biomed Eng Online 1(1):1–7
5. Nagle HT, Gutierrez-Osuna R, Schiffman SS (1998) The how and why of electronic noses. IEEE Spectr 35(9):22–31
6. Korotcenkov G (2012) Chemical sensors applications. Chemical sensors: comprehensive sensor technologies, vol 6. Momentum, New York
7. Chang JB, Subramanian V (2008) Electronic noses sniff success. IEEE Spectr 45(3):50–56
8. Lemmerhirt DF, Wise KD (2006) Chip-scale integration of data-gathering microsystems. Proc IEEE 94(6):1138–1159
9. Boland W, Spiteller D (2001) Electronic noses. In: Hock B (ed) Bioresponse-linked instrumental analysis. Teubner, Stuttgart, pp 57–78
10. Hatfield JV, Neaves P, Hicks PJ, Persaud K, Travers P (1994) Towards an integrated electronic nose using conducting polymer sensors. Sens Actuators B 18(1–3):221–228
11. Arshak K, Moore E, Lyons GM, Harris J, Clifford S (2004) A review of gas sensors employed in electronic nose applications. Sens Rev 24(2):181–198
12. Zee F, Judy JW (2001) Micromachined polymer-based chemical gas sensor array. Sens Actuators B 72(2):120–128
13. Afridi MY, Suehle JS, Zaghloul ME, Berning DW, Hefner AR, Cavicchi RE, Semancik S, Montgomery CB, Taylor CJ (2002) A monolithic CMOS microhotplate-based gas sensor system. IEEE Sens J 2(6):644–655
14. Guo B, Bermak A, Chan PCH, Yan G-Z (2007) A monolithic integrated 4×4 tin oxide gas sensor array with on-chip multiplexing and differential readout circuits. Solid State Electron 51(1):69–76
15. Kim YS, Ha S-C, Yang Y, Kim YJ, Cho SM, Yang H, Kim YT (2005) Portable electronic nose system based on the carbon black–polymer composite sensor array. Sens Actuators B 108(1–2):285–291
16. Hsieh H-Y, Tang K-T (2012) VLSI Implementation of a bio-inspired olfactory spiking neural network. IEEE Trans Neural Netw Learn Syst 23(7):1065–1073
17. Tang K-T, Chiu S-W, Chang M-F, Hsieh C-C, Shyu J-M (2011) A low-power electronic nose signal-processing chip for a portable artificial olfaction system. IEEE Trans Biomed Circuits Syst 5(4): 380–390
18. Koickal TJ, Hamilton A, Su Lim T, Covington JA, Gardner JW, Pearce TC (2007) Analog VLSI circuit implementation of an adaptive neuromorphic olfaction chip. IEEE Trans Circuits Syst I 54(1): 60–73
19. Laconte J, Dupont C, Flandre D, Raskin JP (2004) SOI CMOS compatible low-power microheater optimization for the fabrication of smart gas sensors. IEEE Sens J 4(5):670–680
20. Wang LC, Tang KT, Chiu SW, Yang SR, Kuo CT (2011) A bio-inspired two-layer multiple-walled carbon nanotube–polymer composite sensor array and a bio-inspired fast-adaptive readout circuit for a portable electronic nose. Biosens Bioelectron 26(11):4301–4307
21. Lin Y-W, Wu T-M (2009) Synthesis and characterization of externally doped sulfonated polyaniline/multi-walled carbon nanotube composites. Compos Sci Technol 69(15–16):2559–2565
22. Grate JW, Patrash SJ, Abraham MH (1995) Method for estimating polymer-coated acoustic wave vapor sensor responses. Anal Chem 67(13):2162–2169
23. Wu C-Y, Tang K-T (2010) A polymer-based gas sensor array and its adaptive interface circuit. In: 2010 international symposium on VLSI design automation and test (VLSI-DAT), 26–29 April 2010, pp 355–358
24. Chin S-M, Hsieh C-C, Chiu C-F, Tsai H-H (2010) A new rail-to-rail comparator with adaptive power control for low power SAR ADCs in biomedical application. In: Proceedings of 2010 I.E. international symposium on circuits and systems (ISCAS), May 30–June 2 2010, pp 1575–1578
25. Perera A, Sundic T, Pardo A, Gutierrez-Osuna R, Marco S (2002) A portable electronic nose based on embedded PC technology and GNU/Linux: hardware, software and applications. IEEE Sens J 2(3):235–246
26. Chang M-F, Kwai D-M, Yang S-M, Chou Y-F, Chen P-C (2007) Experiments on reducing standby current for compatible SRAM using hidden clustered source line control. In: 7th international conference on ASIC, 2007. ASICON '07. 22–25 Oct 2007. pp 1038–1041
27. Wilson DM, Hoyt S, Janata J, Booksh K, Obando L (2001) Chemical sensors for portable, handheld field instruments. IEEE Sens J 1(4): 256–274
28. Tang K-T, Chiu S-W, Pan C-H, Hsieh H-Y, Liang Y-S, Liu S-C (2010) Development of a portable electronic nose system for the detection and classification of fruity odors. Sensors 10(10):9179–9193